LUT UNIVERSITY
LUT School of Energy Systems
LUT Mechanical Engineering
BK10A0402 Kandidaatintyö

EFFECT OF THE MOST IMPORTANT PARAMETERS ON PROPERTIES OF INCONEL 718 MANUFACTURED BY LASER POWDER BED FUSION

TÄRKEIMPIEN PARAMETRIEN VAIKUTUS INCONEL 718:N OMINAISUUKSIIN LASERPOHJAISESSA JAUHEPETISULATUKSESSA

Lappeenranta 24.6.2019

Kalle Kohtanen
Examiners Docent Heidi Piili
Advisors Docent Heidi Piili
M. Sc. (Tech) Markus Korpela

TIIVISTELMÄ

LUT Yliopisto
LUT School of Energy Systems
LUT Kone

Kalle Kohtanen

Tärkeimpien parametrien vaikutus Inconel 718:n ominaisuuksiin laserpohjaisessa jauhepetisulatuksessa

Kandidaatintyö

2019

43 sivua, 20 kuvaa ja 1 taulukko

Tarkastaja: Dosentti Heidi Piili

Ohjaaja: Dosentti Heidi Piili
DI Markus Korpela

Hakusanat: Lisäävä valmistus, 3D-tulostus, metalli, laserpohjainen jauhepetisulatus, Inconel 718, energiatiheys, laserteho, skannausnopeus

Tämän kandidaatintyön tarkoituksena oli selvittää tärkeimpien parametrien vaikutus Inconel 718:n ominaisuuksiin laserpohjaisessa jauhepetisulatuksessa. Työ tehtiin kirjallisuuskatsauksena, jossa kerättiin ja koottiin tietoa useista tieteellisistä artikkeleista ja lähteistä.

Työssä valittiin kirjallisuuden perusteella Inconel 718:n laserpohjaisen jauhepetisulatuksen tärkeimmiksi parametreiksi laserteho, skannausnopeus, kerrospaksuus ja skannausviivojen väli sekä näistä laskettava energiatiheys (*VED*, volumetric energy density).

Työssä havaittiin, että Inconel 718:n laserpohjaisessa jauhepetisulatuksessa voidaan todeta olevan neljä erilaista ilmiötä, kun lasersäteen ja materiaalin välistä vuorovaikutusta tarkastellaan. Nämä ovat: avaimenreiän muodostuminen, riittävä sulaminen, epätäydellinen sulaminen ja palloutuminen. Nämä ilmiöt riippuvat paljon käytetystä energiatiheydestä.

Kun käytetään Inconel 718:aa tulostettaessa suurta lasertehoa ja alhaista skannausnopeutta (suuri energiatiheys), muodostuu jauhepetisulatukseen avaimenreikä ja tämän seurauksena valmiin Inconel 718:n pinnanlaatu on huono, mikrorakenne huokoinen ja mekaaniset ominaisuudet ovat alhaiset. Lasertehon ollessa matala ja käytetty skannausnopeus suuri (pieni energiatiheys), jauhepetisulatus on epätäydellisen sulamisen alueella. Inconel 718:n pinnanlaatu, mikrorakenne ja mekaaniset ominaisuudet ovat huonoja johtuen epätäydellisestä sulamisesta, koska kerrokset eivät sulaudu toisiinsa. Kun käytetty laserteho ja skannausnopeus ovat suuria, muodostuu jauhepetisulatuksessa ”palloja” eli ollaan palloutumisen alueella. Inconel 718:n sulamisjälki on epäjatkuva, joka vaikuttaa huonontavasti sen pinnanlaatuun, mikrorakenteeseen ja mekaanisiin ominaisuuksiin.

ABSTRACT

LUT University
LUT School of Energy Systems
LUT Mechanical Engineering

Kalle Kohtanen

The most important input parameters in laser powder bed fusion of Inconel 718

Bachelor's thesis

2019

43 pages, 20 figures and 1 table

Examiner: Docent Heidi Piili

Supervisor: Docent Heidi Piili
M. Sc. (Tech.) Markus Korpela

Keywords: Additive manufacturing, 3D printing, metal, laser powder bed fusion, Inconel 718, volumetric energy density, laser power, scanning speed

Aim of this bachelor's thesis is to find out the effect of the most important parameters on properties of Inconel 718 manufactured by laser powder bed fusion. This thesis is a literature review which was executed by collecting data from several scientific articles and studies.

Based on the literature, the most important parameters of laser powder bed fusion are laser power, scanning speed, layer thickness, hatch and volumetric energy density (*VED*), which can be calculated by previously mentioned parameters.

It was noticed in this thesis that four different phenomena occur when interaction between the laser beam and material was discussed. Those phenomena are: keyhole formation, conduction mode, lack of fusion and balling up. These phenomena depend on the used volumetric energy density and they explain the properties of a final part.

When a large value of laser power and low value of scanning speed (large value of *VED*) are used, a keyhole is formed in the laser powder bed fusion leading to poor quality of surface, to porous micro structure and to poor mechanical properties of Inconel 718. When a low value of laser power and large value of scanning speed (low value of *VED*) are used, the zone is lack of fusion. In this zone, the quality of surface, micro structure and mechanical properties suffer from the lack of fusion because the poorly molten layers do not bond to each other. When both values, laser power and scanning speed, are large, the zone is balling up and large beads starts to occur. Then the scan track is discontinuous, and it results to poor quality of surface, porous micro structure and low values of mechanical properties of Inconel 718.

ACKNOWLEDGEMENTS

This study was carried out in co-operation with company Etteplan and research group of Laser Material Processing of LUT University as a part of Metal 3D Innovations (Me3DI) project funded by European Regional Development Fund. Aim of Metal 3D Innovations-project (Me3DI) is to form industrial knowhow cluster of metallic 3D printing to South Karelia. This cluster will enhance utilization of additive manufacturing (3D printing) of metallic materials. This project is funded by European Regional Development Fund. Project started in 1.9.2018 and ends in 31.12.2020. Research group of Laser Materials Processing and research group of Steel Structures of LUT University and industrial companies are participating into this project.

I would like to thank Etteplan, especially my contact persons Johannes Karjalainen and Antti Suikki, for giving me the opportunity for doing this thesis. It was a pleasure to do my bachelor's thesis on such an interesting topic!

I also want to thank my supervisors Docent Heidi Piili and researcher Markus Korpela for helping and supporting me through making of this thesis.

Kalle Kohtanen

Kalle Kohtanen

Lappeenranta 2019

TABLE OF CONTENTS

LIST OF SYMBOLS AND ABBREVATIONS

h	hatch spacing [mm]
LED	linear energy density [J/mm]
P	laser power [W]
R_a	average roughness of the surface (profile measurement)
S_a	average roughness of the surface (areal measurement)
t	layer thickness of powder bed [mm]
v	scanning speed [mm/s]
VED	volumetric energy density [J/mm^3]

3D	Three-dimensional
AM	Additive Manufacturing
CAD	Computer-aided Design
L-PBF	Laser Powder Bed Fusion
Me3DI	Metal 3D Innovations
PBF	Powder Bed Fusion
STL	STL file format

1 INTRODUCTION

Additive manufacturing (AM) contains multiple technologies that use computer aided design (CAD) data to form physical shapes (Gibson, Rosen & Stucker 2015, p. 1; Gu 2015, p. 1). The general principle of AM is to add material only to locations where it is needed, unlike in the conventional manufacturing where the material is removed from a material blank to achieve the desired geometry. (Gibson et al. 2015, p. 2.) Generally, AM sales have been growing fast in recent years (Wohlers 2019, p. 164). Figure 1 represents the general growth of AM sales, including all AM technologies.

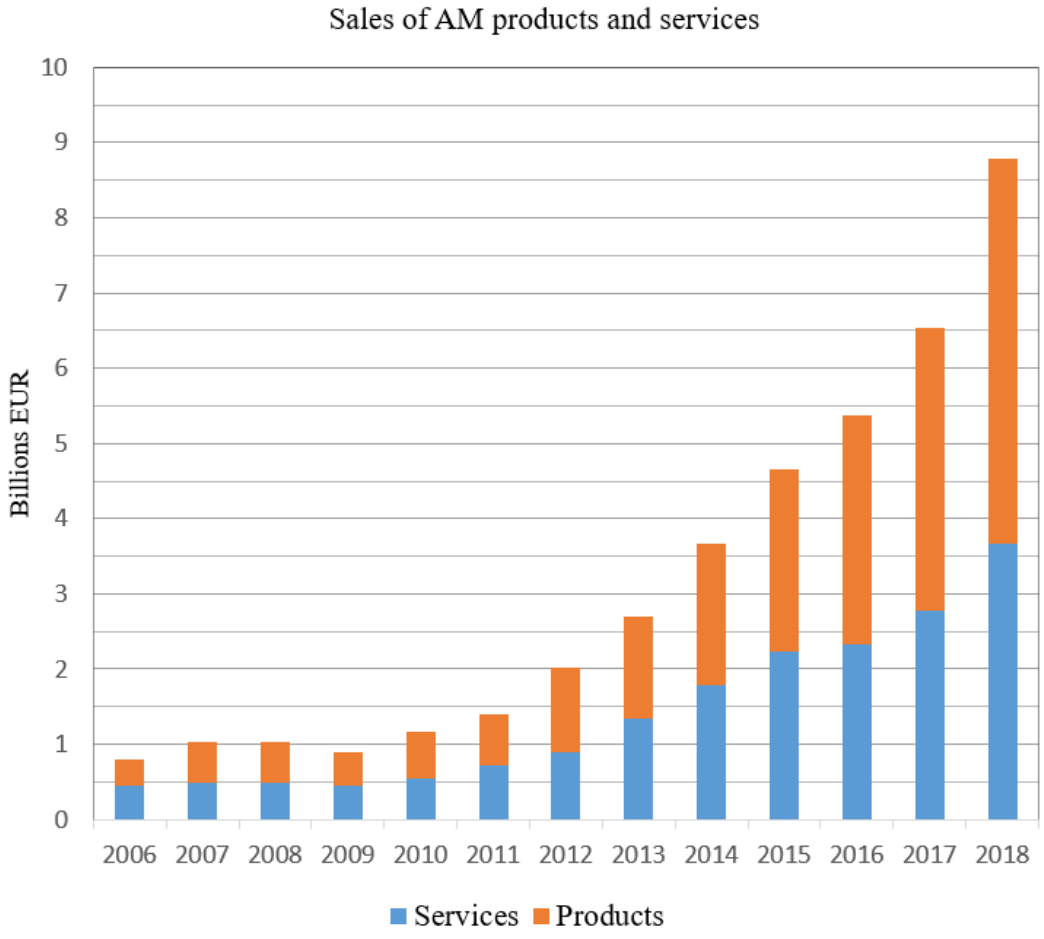

Figure 1. The global sales of AM services and products, when all AM technologies are considered (mod. Wohlers 2019, p. 164.)

As it can be seen from Figure 1, the sales of AM services and products have increased tenfold from 2006 to 2018. In 2006, the sales size was under 1 billion Euros. The same number in 2018 was more than 8.5 billion Euros. (Wohlers 2019, p. 164.) Figure 2 indicates the global sales of metal AM systems.

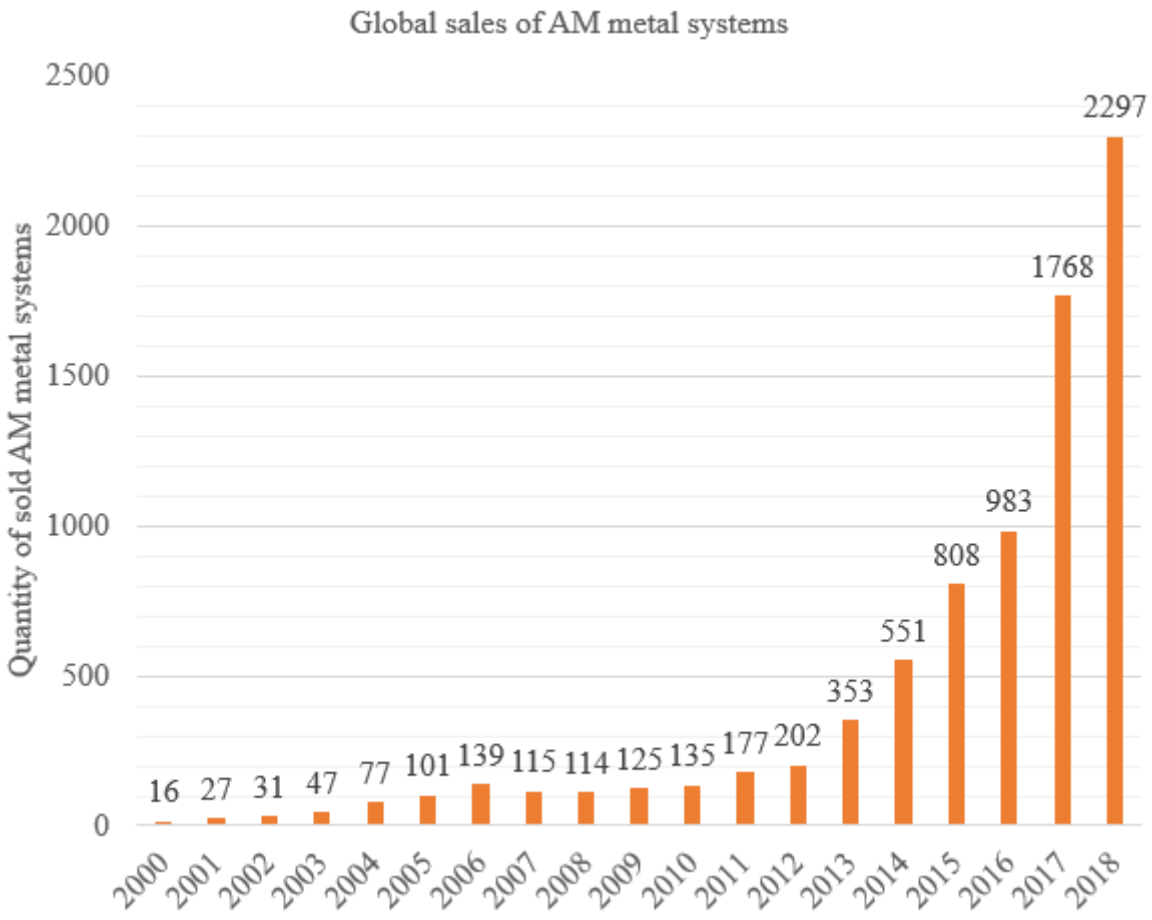

Figure 2. The global sales of metal AM systems (mod. Wohlers 2019, p. 169.)

As it can be observed from Figure 2, the quantity of sold AM metal systems is globally increasing fast. Even the growth in sales of AM metal systems in 2018 (2297) over the 2017 (1768) was almost 30%. (Wohlers 2019, p. 169.)

The range of useable materials in AM is nowadays wide. There are seven existing standardized AM processes (Gibson et al. 2015, p. 35):

1) vat photopolymerization
2) powder bed fusion
3) material extrusion
4) material jetting
5) binder jetting
6) sheet lamination
7) directed energy deposition.

All the standardized processes can fabricate metallic materials, except vat photopolymerization (Gibson et al. 2015, p. 51–52). Powder bed fusion (PBF) is the most often used AM process for metallic materials due to its accuracy (Donmez et al. 2015, p. 527). Therefore, this thesis focuses on PBF, especially on laser-based powder bed fusion (L-PBF).

This thesis was made in co-operation with company of Etteplan and research group of Laser Materials Processing of LUT as a part of Metal 3D Innovations (Me3DI) project. Aim of Metal 3D Innovations-project (Me3DI) is to form industrial knowhow cluster of metallic 3D printing to South Karelia. This cluster will enhance utilization of additive manufacturing (3D printing) of metallic materials. This project is funded by European Regional Development Fund. Project started in 1.9.2018 and ends in 31.12.2020. Research group of Laser Materials Processing and research group of Steel Structures of LUT University and industrial companies are participating into this project.

Etteplan is a company that provides solutions for the largest companies in the field of manufacturing technology. Etteplan employs more than 3000 professionals in Europe and China.

1.1 Aim of the thesis, research problem and questions

Aim of this thesis is to find the effect of most common parameters on properties of Inconel 718, when laser powder bed fusion (L-PBF) is used. Research problem is to define which parameters of L-PBF need to be used to achieve a satisfying quality of Inconel 718 fabricated by L-PBF. Figure 3 shows the published articles from 2014 to 2019 relating to the topic of this thesis.

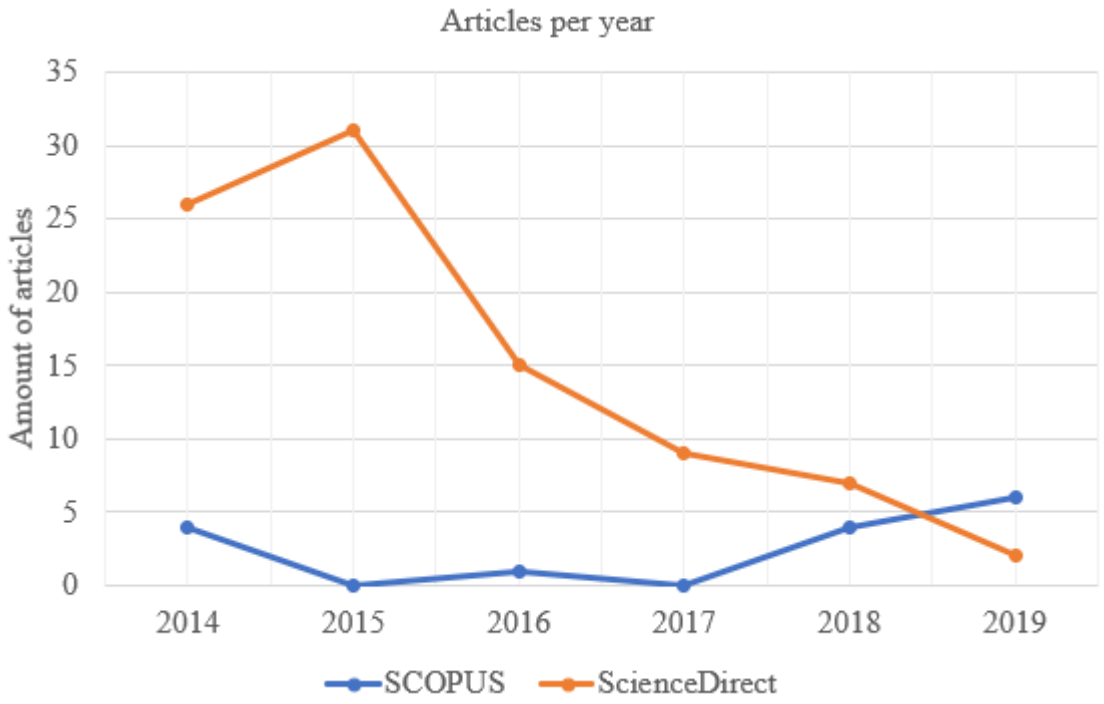

Figure 3. Published articles in SCOPUS and ScienceDirect databases in years 2014-2019 related to topic of this thesis.

As Figure 3 shows, number of published articles is low, varying between 9 and 31 publications per year. The red line indicates the amount of publications in ScienceDirect and the blue line shows the quantity of publications in SCOPUS. Also, only one company in Finland offers L-PBF of Inconel 718 (Korpela 2019, p. 28). This is why, this thesis will provide new insight and collected information to this field of additive manufacturing. This also has been one of motivations to carry out this thesis.

The research questions are:

- How can the parameters of L-PBF be classified?
- Which are the most important parameters in L-PBF of Inconel 718?
- Which are most important properties of Inconel 718 manufactured by L-PBF?
- How does the changing of the main parameters affect the quality of Inconel 718 fabricated by L-PBF?

1.2 Research methods and framing

This thesis was conducted as a literature review utilizing literature sources from LUT Finna and Google Scholar. In this thesis, the most important parameters in L-PBF of Inconel 718 and most important properties of Inconel 718 are studied, as well as effect of the parameter change on Inconel 718 is discussed.

It was decided to frame the topic of the thesis to process of L-PBF and to material of Inconel 718. The reason for choosing L-PBF as a process is that it is the most popular process of AM of metals (Wohlers et al. 2019, p. 188). Inconel 718 was chosen because not so many articles of L-PBF of Inconel 718 exist, as it can be seen from Figure 3. Also, Etteplan showed an interest towards this material.

2 LASER POWDER BED FUSION

Powder bed fusion (PBF) is one of the processes of additive manufacturing (AM). A few types of PBF processes exist but this thesis focuses on laser powder bed fusion (L-PBF). (Ashraf, Gibson & Rashed 2018, p. 3.) Generally, lasers are used as a principal thermal source for PBF, but electron beam can be used as well (Gibson et al. 2015, p. 136).

Plastics, ceramics and metals can be manufactured by L-PBF. However, this thesis focuses on metals, specifically on Inconel 718 alloy. Basically, every fusion weldable material can be used in L-PBF. (Gibson et al. 2015, p. 109.)

2.1 Basics of modelling

L-PBF process starts by creating a 3D model of a part. The 3D model can be created by several different CAD software. Scanning technology (aka reverse engineering) can be exploited when creating the 3D model but it has to be noted that scanning only produces model of the outer surface of a model. 3D model must be converted into a STL file format, or some other format which presents the 3D model by vectors, so the AM system is able to read the data. (Gibson et al. 2015, pp. 4–5; Gu 2015, pp. 4–6.) Support structures are needed if the manufactured material is metal. Melting points of metals are high and too large differences in temperatures cause thermal stresses and warping on the final parts manufactured by L-PBF. It can be solved by anchoring structures below the part for conducting the heat away. In addition, the supports are used to keep part attached into building platform. (Wohlers et al 2018, p. 41.) After the conversion into suitable file format, the model will be sliced into multiple thin 2D cross-section layers by using a slicing software. The sliced model file will be transferred to the L-PBF machine and there it is possible to do the final adjusting to position of model on the building platform and for example size of the model. Next step is to set the process parameters such as scanning speed and power of the thermal source. (Gibson et al. 2015, pp. 4–5; Gu 2015, pp. 4-6.)

2.2 Basics of laser powder bed fusion process

L-PBF process contains a few simple steps which will be repeated as many times as there are layers in the sliced model (Atwood et al. 2018, p. 648; Gu 2015, p. 6). The mechanism of L-PBF is illustrated in Figure 4.

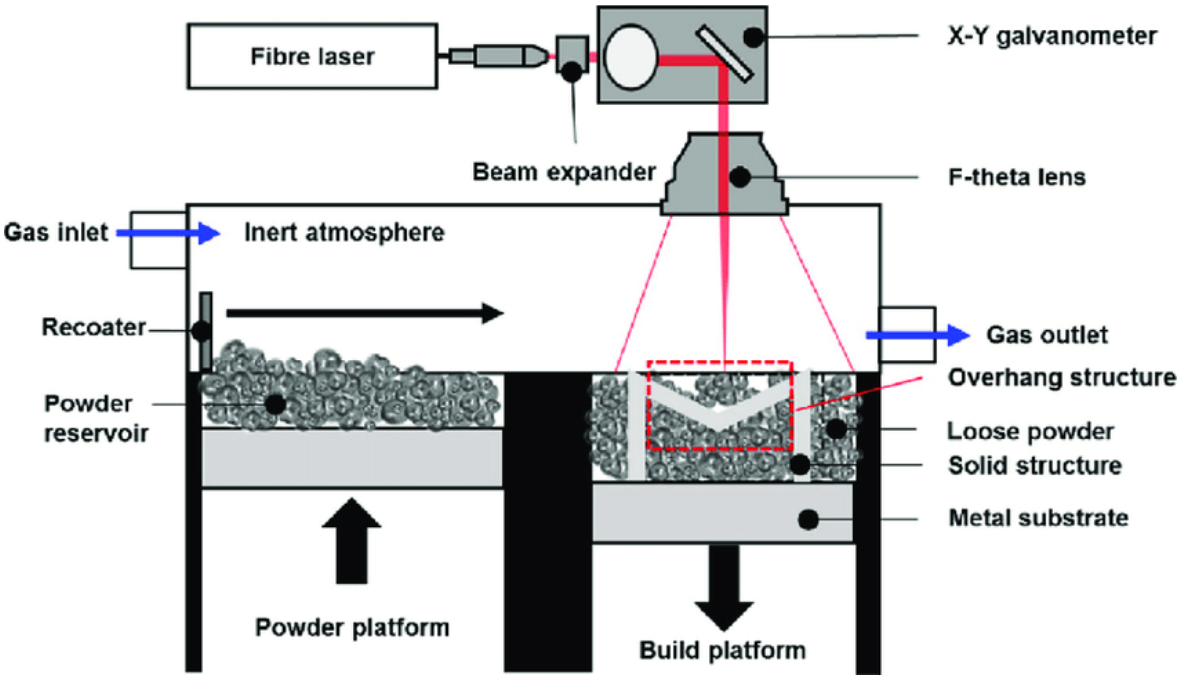

Figure 4. Schematic of L-PBF mechanism (Atwood et al. 2018, p. 648).

As it can be seen in Figure 4, recoater blade spreads first the powder from powder reservoir onto the building platform. The black arrow shows the direction of the spreading. The powder can be spread by roller but recoater blade is more commonly used. Once the powder is spread, the laser melts the cross-section of the sliced model on the powder layer. Build platform is then pulled down for a height of the next layer. New layer of powder is spread after this from the powder reservoir by using the recoater blade. These steps make a loop that will be repeated until the piece is completely ready. (Atwood et al. 2018, p. 648; Nai et al. 2017, p. 700.) Inert gas, such as nitrogen, is used in the building chamber to prevent oxidation, degradation and discoloration (Milewski 2017, p. 241). Finished piece is surrounded by unmelted powder, which will be removed. After accurate handling and sieving, most powder can be recycled and reused. Therefore, L-PBF process has a low waste ratio. (Nai et al. 2017, p. 700.) The basic principle of PBF process can be seen in Figure 5.

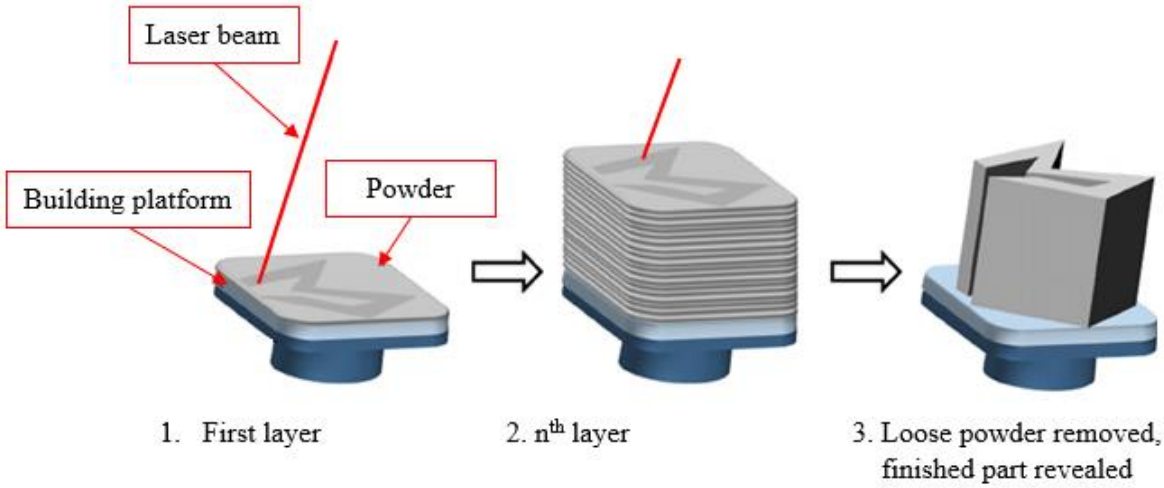

Figure 5. L-PBF process in three steps (mod. Chua et al. 2015, p. 2).

As it can be seen from Figure 5, a building platform mis above the moving base platform and the laser melts the area of the cross-section to the powder layer multiple times layer by layer. The loose powder is removed around the part in the last step. (Chua et al. 2015, p. 2.) After removal of the powder, finished part will be cut off the build platform (Gibson et al. 2015, p. 48).

3 INCONEL 718

Inconel is a product family of nickel-based alloys made by Special Metals Corporation and Inconel 718 is a trade name of one alloy in that product family. It is called a superalloy due to its mechanical properties which are introduced later in this Chapter. Inconel 718 has applications in various fields of technology. It is in common use for example in aerospace applications, gas turbines and as a cladding material due to its mechanical properties. (Milewski 2017, p. 70; Special Metals 2007, p. 1.)

Inconel 718 is not the most appropriate material for conventional machining due to high shear strength, poor thermal conductivity and low material removal rate. These characteristics cause high costs and power consumption in conventional machining. Because the conventional machining is not effective, Inconel 718 is more often used in L-PBF process as PBF is tool-free process. It must be noted that also parts manufactured by L-PBF often needs to be machined to achieve a satisfying quality (Gibson et al. 2015. p. 6). For example, polishing and removing the support structures are often needed (Baughman et al. 2017. p. 42; Gibson et al. 2015. p. 325). High shear strength can cause difficulties in this post-processing phase. (Special Metals 2007, p. 26.)

As mentioned in the Chapter 2, the unused powders in L-PBF process can be recycled well. This leads into a low material waste, which is important when manufacturing parts are made of expensive superalloys such as Inconel 718. (Alfieri et al. 2017, p. 4023; Arrazola et al. 2016, p. 441.)

Inconel 718 contains many different alloying components in addition to nickel. The composition limits of the alloy can be seen in Table 1. The most dominant components in Inconel 718 are nickel, chromium and iron. (Special Metals 2007, p. 2.)

Table 1. Limits of the chemical composition of Inconel 718 (mod. Special Metals 2007, p. 2).

Composition	Weight %
Nickel (plus Cobalt)	50.00–55.00

Table 1 continues. Limits of the chemical composition of Inconel 718 (mod. Special Metals 2007, p.2).

Chromium	17.00–21.00
Iron	Balance (the rest part of the total count)
Niobium (plus Tantalum)	4.75–5.50
Molybdenum	2.80–3.30
Titanium	0.65–1.15
Aluminum	0.20–0.80
Cobalt	max. 1.00
Carbon	max. 0.08
Manganese	max. 0.35
Silicon	max. 0.35
Phosphorus	max 0.015
Sulphur	max. 0.015
Boron	max. 0.006
Copper	max. 0.30

As Table 1 shows, the quantity of iron is significant which means Inconel 718 can be hardened with heat treatments. Inconel 718 can be welded easily and cracking after cooling is minimal. Inconel 718 has good tensile strength properties in high temperatures. In addition, creep properties and corrosion resistance of Inconel 718 makes it a notable material in the fields of technology where good material properties are needed. This kind of applications are for example bolts and nuts used in high temperatures, rocket engine parts and turbine parts. (Special Metals 2007, p. 2)

4 CATEGORIZATION OF PARAMETERS OF LASER POWDER BED FUSION

The parameters in L-PBF process can be classified in several ways. This thesis introduces two of them.

4.1 Laser beam and material interaction diagram

According to Piili (2012, p. 114), parameters in laser processing generally can be classified for three different groups: input parameters, output parameters during interaction and output parameters. Figure 6 illustrates this parameter division by means of laser beam and material interaction. (Piili 2012, p. 114.)

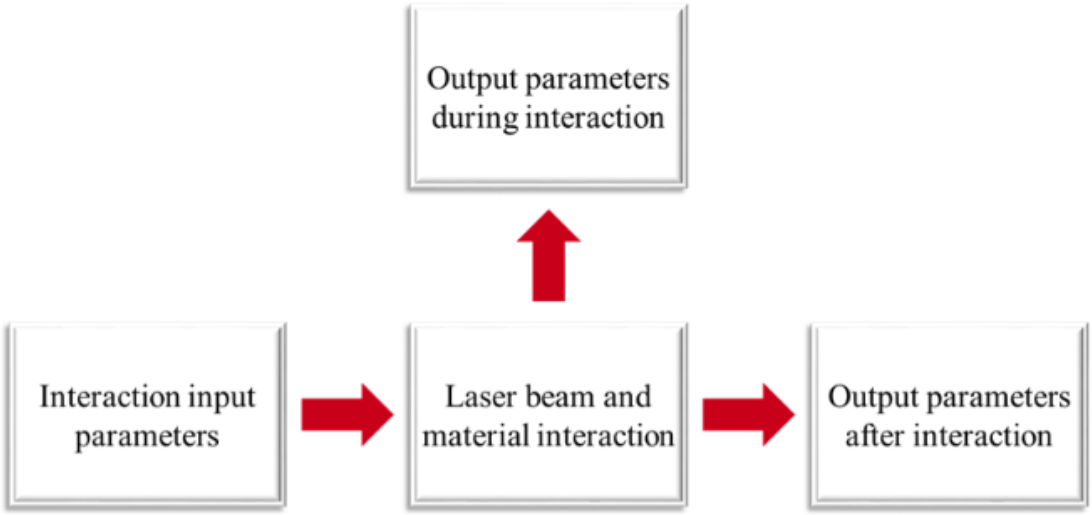

Figure 6. Laser beam and material interaction diagram (Piili 2012, p. 114).

As Figure 6 shows, every parameter type has relation with the laser beam and material interaction. Input parameters are all those parameters which are adjusted before the laser beam and material interaction. Parameters during or after the interaction are output parameters. Basic characteristics for this diagram shown in figure 6 is that all parameters are related to each other's. (Piili 2012, p. 114.) This thesis focuses only on input parameters. Input parameters can be divided into three sub-parameters and these are shown in Figure 7.

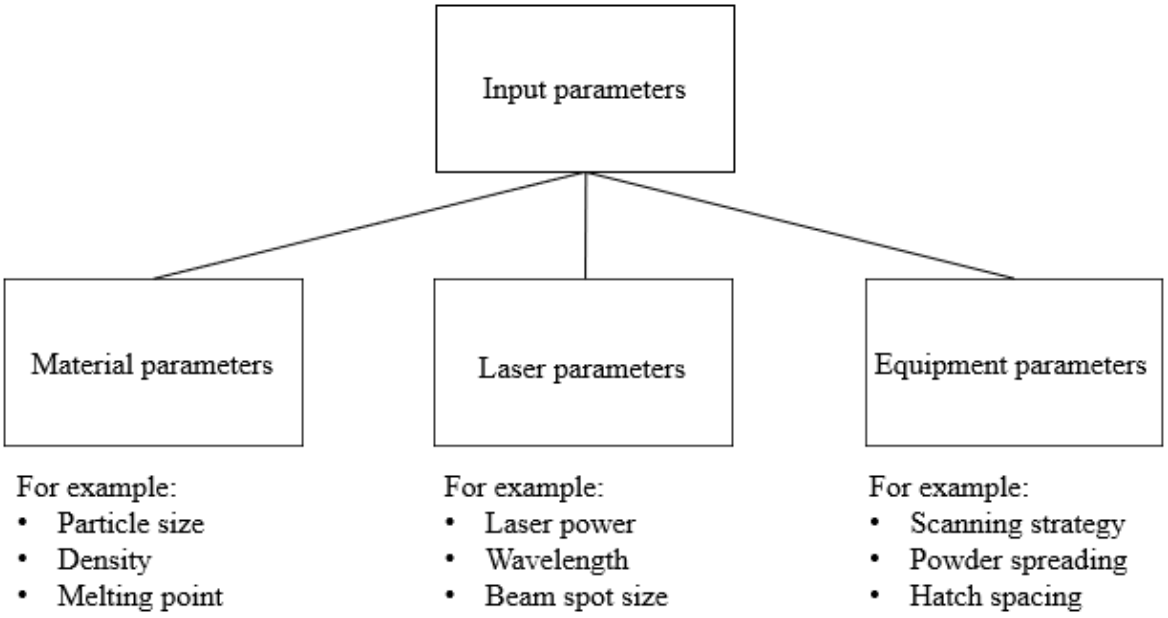

Figure 7. Diagram of the input parameters in L-PBF (Piili 2019).

As Figure 4 represents, input parameters can be categorized into three groups: 1) material parameters, 2) laser parameters and 3) equipment parameters. Material parameters include all material related parameters, such as material density and particle size of the material. Laser parameters mean all parameters which are related to laser beam, and they are for example, laser power and spot size of the beam. Equipment parameters are all those parameters which determine the characteristics of process and system, such as recoater speed. (Piili 2019**)**

4.2 Ishikawa diagram

Another way of categorizing the L-PBF parameters is an Ishikawa diagram (Carty et al. 2018, p. 29). Basic principle in this division is to find the effects and causes of a process. Usually there are 4-6 groups which presents different kind of causes, for example (Liliana 2016, p. 3.):

1) man/personnel
2) methods
3) materials
4) machines
5) environment.

Next step is to determine the effects and errors, which those 4-6 groups cause. The effects and errors can be very accurate, for example effects in micro hardness or effects in formation of pores of a manufactured part. In addition, the effects can be very generic, for example effects in quality or general accuracy of a manufactured part. An example of Ishikawa diagram that are adapted into L-PBF can be seen in Figure 8. (Liliana 2016, p. 3.)

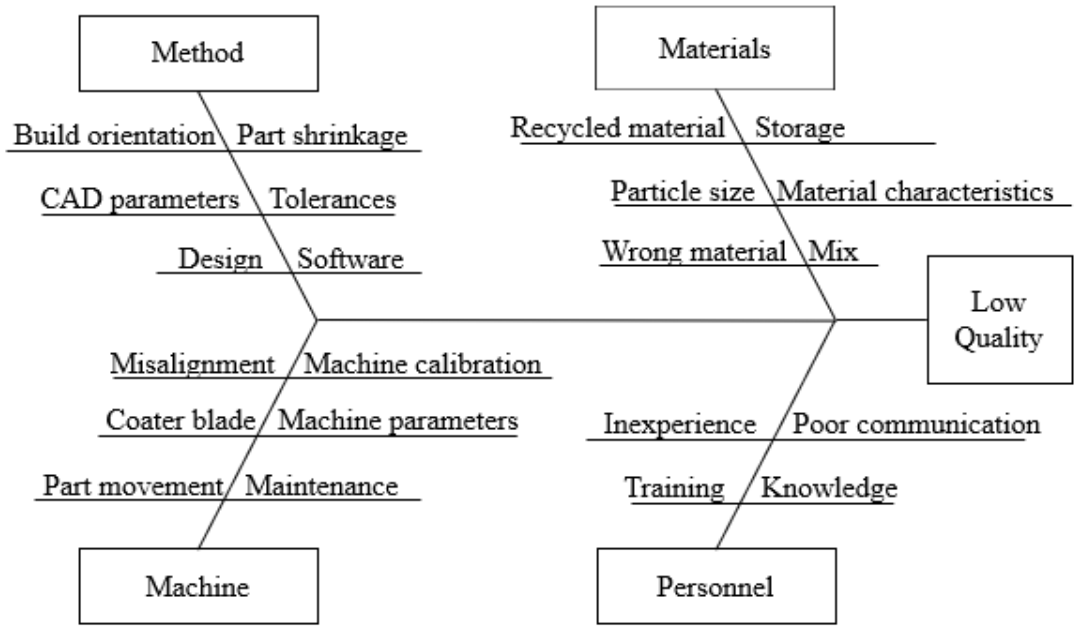

Figure 8. Ishikawa diagram of L-PBF parameters (mod. Carty et al. 2018, p. 29).

As it can be seen from Figure 8 the main parameter groups are divided onto four main groups: 1) materials, 2) method, 3) machine and 4) personnel. Material parameters are all parameters which are somehow related to the material, for example if it is totally wrong material for the process or poor particle size. Machine parameters are all those parameters which can be adjusted by the L-PBF machine and its software, for example localized heating and beam spot size. Method parameters are the parameters related how the model is made, for example which CAD-software is used and how the part is designed. Problem with this diagram is that it is inefficient by means of understanding which parameters effect quality of part i.e. this model does not take into account the laser beam and material interaction. (Carty et al. 2018, p. 29.)

5 MAIN INPUT PARAMETERS IN L-PBF

This Chapter introduces following most common parameters in L-PBF process (Austbø et al. 2018, p. 910; DebRoy & Mukherjee 2018, p. 442):

- laser power
- scanning speed
- layer thickness
- hatch spacing.

It was decided in this thesis to use value of volumetric energy density (*VED*), because it combines all above mentioned common parameters into one single value. In addition, *VED* is commonly used value in the scientific studies of L-PBF (Bertoli et al. 2017; Emmelmann et al. 2016, p. 372; Gu 2015, p. 60; Guo et al. 2018, p. 483).

VED can be calculated as equation 1 shows (Bertoli et al. 2017; Emmelmann et al. 2016, p. 372; Gu 2015, p. 60; Guo et al. 2018, p. 483.):

$$VED = \frac{P}{v \times h \times t} \quad (1)$$

In Equation 1 *VED* is volumetric energy density (J/mm^3), *P* is laser power (W), *v* is scanning speed (mm/s), *h* is hatch spacing (mm) and *t* is layer thickness (mm). The parameters of *VED* are introduced in Figure 9.

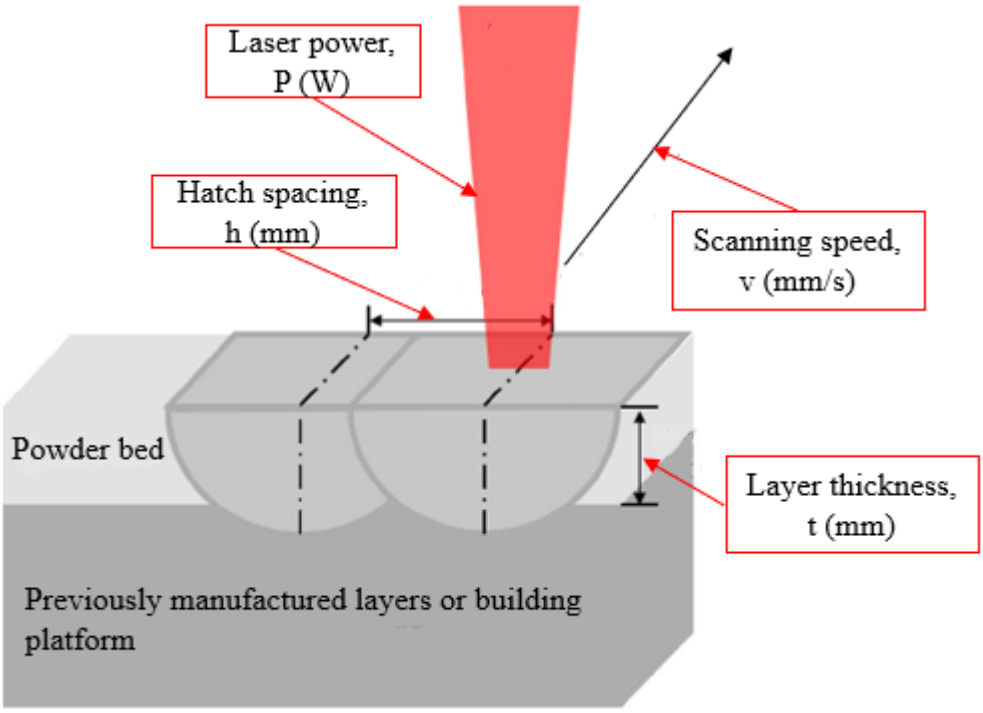

Figure 9. Parameters of *VED* (Chua et al. 2015, p.3).

As it can be seen from Figure 9, hatch spacing is the distance between the scan lines which are formed by the laser beam (Gibson et al. 2015, p. 390). Too long hatch spacing leads to poor melting between scan lines (i.e. low local value of energy density) because the distance of scans is too long and the fusion between scans does not happen. Scanning speed is the speed of laser beam when it travels on the powder bed. The speed must be optimized properly in L-PBF process. Too slow scanning speed can cause vaporization and other defects to ready workpiece because the long interaction time between laser beam and material brings too much energy to the material (Qi et al. 2017, p. 258). When too much energy is brought to a material, the temperature increases over the melting point. Too high temperature leads to spattering melt pool and boiling metal which cause decreasing in the quality of a part manufactured by L-PBF (Saunders 2017). On the other hand, too high scanning speed leads to too short interaction time between the beam and the powder bed and the powder will not melt properly. (Chua et al. 2015, p. 3) Figure 10 illustrates how pores can be visible and how it depends on the scanning speed.

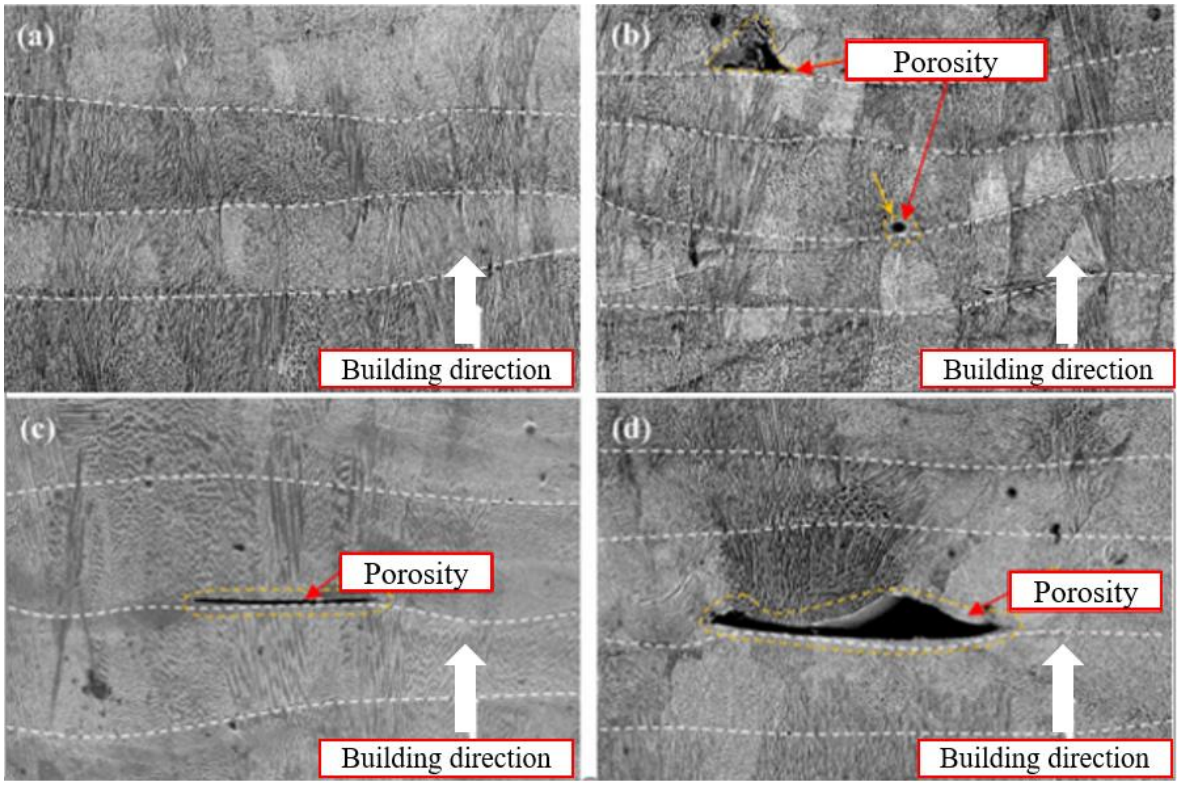

Figure 10. Porosity formation of Inconel 718 with different values of scanning speed: (a) 200 mm/s, (b) 300 mm/s, (c) 400 mm/s, (d) 500 mm/s. Constant value of laser power was used in all tests. (mod. Chen et al. 2017, p. 104.)

As Figure 10 shows, four different samples (10a, 10b, 10c and 10d) for four different scanning speed values (200 mm/s, 300 mm/s, 400 mm/s and 500 mm/s) were manufactured. Chen et al. (2017) do not mention value of laser power in their study but constant value of laser power was used in all tests. White arrow shows the building direction. The interaction time between laser beam and the material is the longest with value of 200 mm/s (Figure 10a) and shortest with value of 500 mm/s (Figure 10d). Due to relatively short interaction times, the formation of pores is visible in tests made with values of 300 mm/s (Figure 10b), 400 mm/s (Figure 10c) and 500 mm/s (Figure 10d). The largest pore is on the test made with value of 500 mm/s, because the interaction time has been too short, and the material has not molten properly. (Chen et al. 2017, p. 104.) The Figure 11 illustrates how the formation of pores happen.

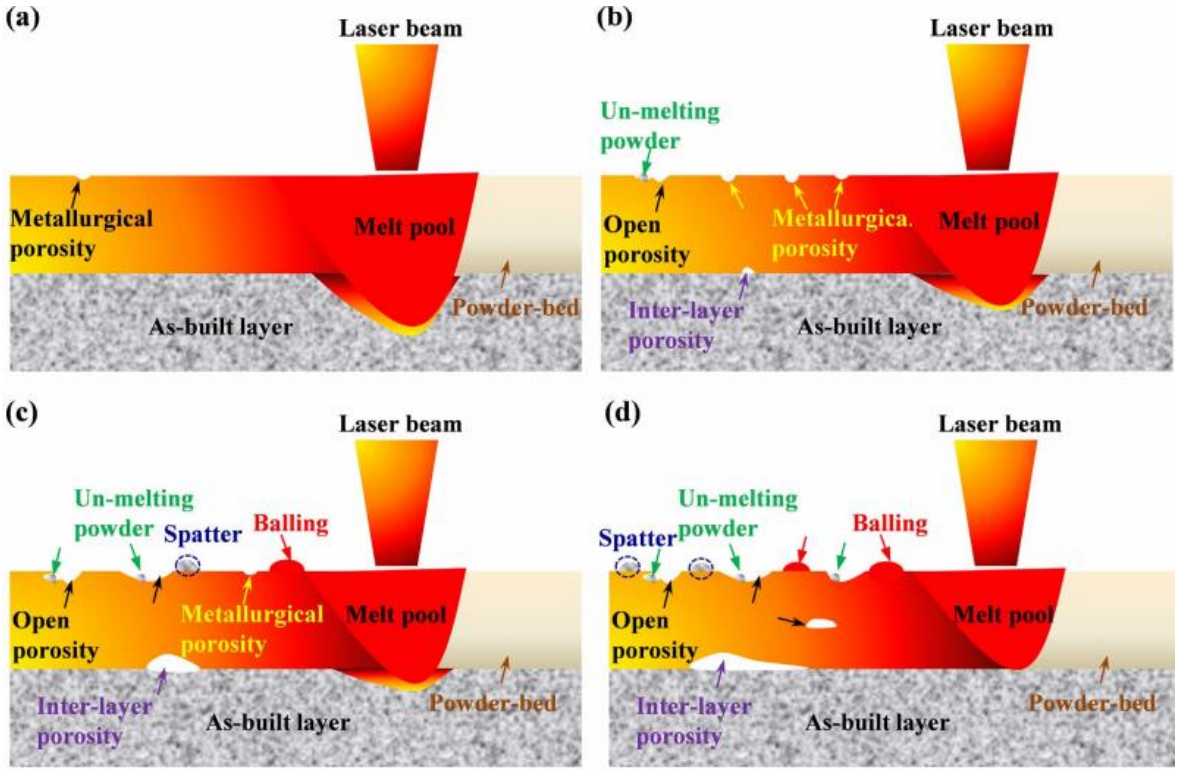

Figure 11. Principle of the formation of the pores with different values of scanning speed: (a) 200 mm/s, (b) 300 mm/s, (c) 400 mm/s, (d) 500 mm/s Constant value of laser power was used in all tests. (Chen et al. 2017, p. 104.)

As it can be seen from Figure 11, the material is molten properly when scanning speed of 200 mm/s (Figure 11a) is used. Chen et al. (2017) do not mention value of laser power in their study but constant value of laser power was used in all tests. It can be observed from Figure 11a that only small amount of metallurgical porosity can be noticed on the surface of solidified track. The melt pool is large because enough energy is brought to the material, so that melt pool is in contact with previously molten layer. When this happens, the both layers are attached to each other and heat from melt pool can be conducted away. When scanning speed of 500 mm/s (Figure 11d) is used, disturbances in melting can be observed. The melt pool is not in contact with previously molten layer, so heat can only be conducted into direction of recently molten track. This leads to overheating and causes disturbances in cooling of track. When the metallurgical bond has not been formed, the pores form between the layers. If the melt pool is as shallow as shown in Figure 11d, there may occur some unmolten powder between molten track and previously manufactured layer. The unmolten powder is also result of too high scanning speed and melt pool might also spatter the

unmolten powder (Wang et al. 2017, p. 124). Also, balling can be observed when scanning speed values is 400 mm/s and 500 mm/s. (Chen et al. 2017, p. 104.) The balling occurs when the melt pool becomes unstable due to too high scanning speed. In addition, too slow scanning speed with large value of laser power cause balling and spattering because material starts to vapour and the melt pool starts to roil. (Saunders 2017; Wang et al. 2017, p. 124.) These issues will be further introduced later in this Chapter.

Layer thickness is the height of the spread powder layer. Thin layers increase the overall production time but does not reduce the material properties such as tensile and hardness properties. If powder layer is too thick, this can lead to non-desired material properties, such as poor tensile strength. The reason for that is when the powder layer is too thick, the melt pool cannot penetrate to previously molten layer as it can be seen in Figure 11. (Borisov et al. 2016, p. 133; Chen et al. 2017, p. 104.)

Saunders (2017) published a division of different laser beam and material interaction zones in L-PBF when scanning speed is represented as function of laser power. The division can be seen in Figure 12.

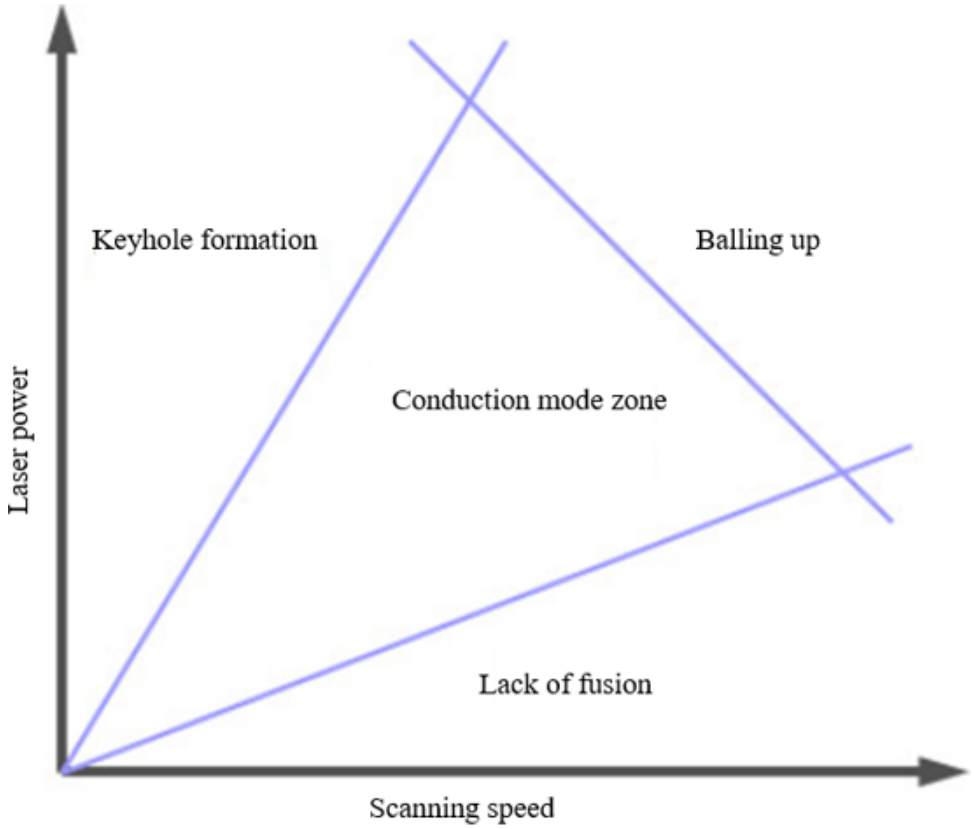

Figure 12. Different laser beam and material interaction zones when scanning velocity is represented as function laser power (Saunders 2017).

As it can be seen from Figure 12, laser beam and material interaction is divided in four zones: conduction mode, lack of fusion, keyhole formation and balling up. Optimal interaction zone is conduction mode, when values of scanning speed and laser power can be controlled. It means that the relation between laser power and scanning speed are constant and no harmful defects, such as pore formation and spattering, occur. This is because circumstances in melt pool are stable. When scanning speed is increased and value of laser power is low, interaction zone is lack of fusion. This results too shallow melt pool which does not reach previously fabricated layer. Lack of fusion is demonstrated in Figure 11d. (Saunders 2017.) When scanning speed is low and laser power is increased, interaction zone is keyhole formation due to excess amount of energy present in laser beam and material interaction (Qi et al. 2017, p. 258). The keyhole formation is illustrated in following Figure 13.

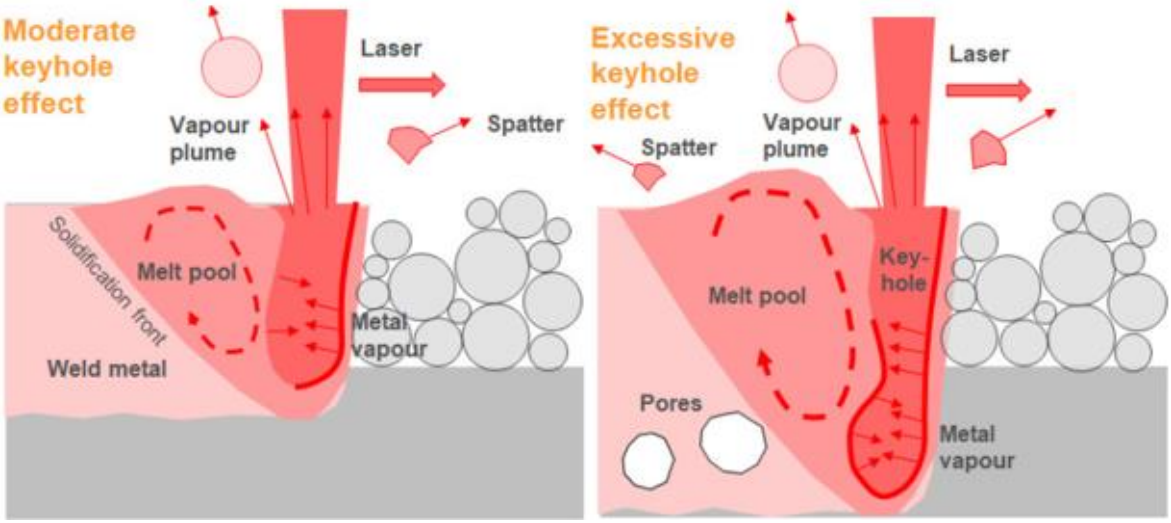

Figure 13. Formation of keyhole and keyhole effect in L-PBF (mod. Saunders 2017).

As it can be seen from Figure 13, two kind of keyhole effect occur: moderate keyhole effect and excessive keyhole effect. The moderate keyhole effect is formed, when scanning speed is low and laser power is increased. The temperature of metal increases so much that metal starts to vapour and the vapour vortex creates an open cavity. The melt pool loses its stability and start to roil and spatter. (Saunders 2017; Wang et al. 2017, p. 124.) Spatters are molten metal particles which are ejected from the melt pool due to its instability and roiling. The excessive keyhole effect is basically made in the same way as moderate keyhole effect: too much energy is brought to a material, but the value of laser power is now increased much more than the value of scanning speed. Also, the melt pool collapses in the cavity resulting a deeper penetration into previous molten layer than the moderate keyhole effect does. In addition, the defects occur stronger (Qi et al. 2017, p. 258; Wang et al. 2017, p. 124). Because the melt pool is now larger, more unstable and its penetration depth is larger, it melts “holes” on the previously fabricated layer i.e. process is not anymore melting but closer to keyhole welding (Qi et al. 2017, p. 258). When the melt pool solidifies, pore might appear due to high instability of melt pool. In addition, both cases have very poor surface quality and high surface roughness. (Saunders 2017; Saunders 2018.)

As it can be seen from Figure 9, when scanning speed and laser power has large value, interaction zone is balling up. The phenomenon is illustrated in following Figure 14.

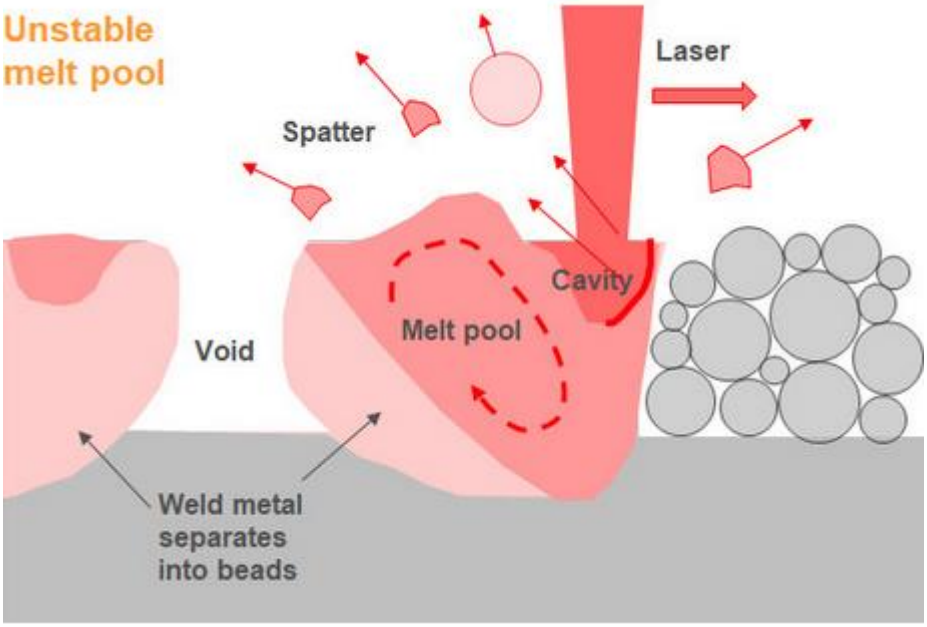

Figure 14. Balling up interaction zone (Saunders 2017).

As it can be seen from Figure 14, melt pool can be unstable when high scanning speed and low laser power is used. In addition to spattering, when the melt pool is unstable, and it creates the cavity below the beam, pores starts to occur due to high surface tension gradients. (Saunders 2017.) When the scanning speed is high, and material has no time to melt properly i.e. to form proper melt pool, the pores behind the laser beam extend and generate voids resulting a discontinuous track (Li et al. 2012, p. 1031; Saunders 2017).

6 EFFECT OF *VED* ON PROPERTIES OF INCONEL 718

When *VED* value is adjusted, it has effects to properties of Inconel, such as (Moussaoui et al. 2018, p. 183):

- quality of the surface
- microstructure of the final part
- mechanical properties of final part.

Change in the surface quality is for example surface roughness. Microstructure changes are for example changes in the dendrites and changes in density. Several mechanical properties exist, but in this thesis, focus is on tensile properties. (Moussaoui et al. 2018, p. 183.) These properties are chosen to be considered to be further discussed in this thesis, because they are often mentioned in the scientific articles and studies relating to the topic of this thesis. **(**Chen et al. 2018, p. 952; Feng et al. 2018, p.485; Moussaoui et al. 2018, p. 183.**)**

6.1 Effect on surface quality

Main quantity to describe the surface quality is surface roughness. It can be defined as an average height difference between the microscopic deviations on the surface. (Arroyave et al. 2018, p.625) Usually, the most used symbol for surface roughness is R_a and it is used for profile measurements. Figure 15 presents surface roughness (S_a) of Inconel 718 as function of scanning speed and laser power. The main difference between Sa and R_a is that S_a is used for measurements for area of surface.

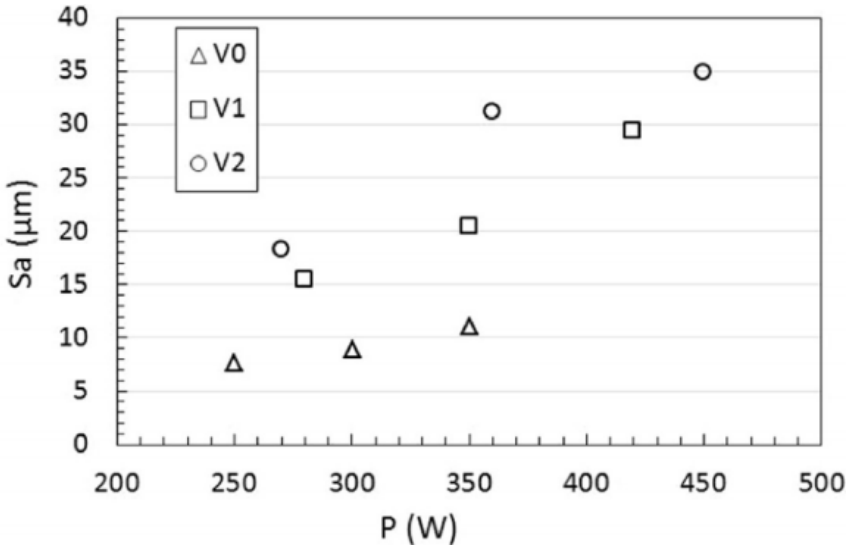

Figure 15. Surface roughness of Inconel 718 fabricated by L-PBF as function of laser power. V0, V1 and V2 are different values of scanning speed. V0 is the smallest value and V2 is the largest value. (Moussaoui et al. 2018, p.184)

According to Moussaoui et al. (2018 p. 184) laser power and scanning speed influence on surface roughness as it can be observed from Figure 15. Surface roughness increases as function of laser power. When laser power is increased from 250 W to 350 W and scanning speed is constant (V0), surface roughness values increases from 6.7 micrometers to 11 micrometers. Due to these changes, melt pool is larger and deeper and because of this more unstable causing spattering and balling (keyhole effect, see Figure 13) (Kivirasi et al. 2017, p. 4; Saunders 2017).

On the other hand, the change of surface roughness depends also on the scanning speed. Increase in scanning speed is increasing surface roughness. For example, when laser power is 350 W and scanning speed is V0 and V1, surface roughness value is 10 micrometers larger with scanning speed of V1 than with scanning speed of V2. Scanning speed affects to surface roughness, because when the value of scanning speed is too large, the melt pool does not reach the previously manufactured layer as it can be seen in Figure 11d (Chen et al. 2017, p. 104). (Moussaoui et al. 2018. p. 184.). Figure 16 presents the surface roughness of Inconel 718 as function of *VED*.

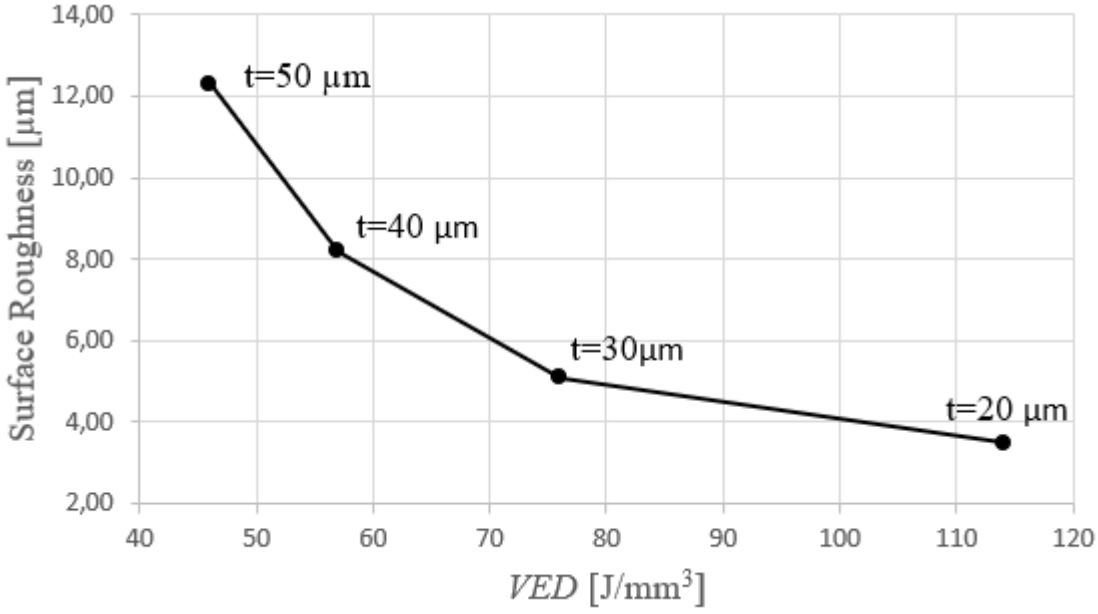

Figure 16. Surface roughness of Inconel 718 fabricated by L-PBF as a function of *VED*. Constant values of scanning speed, hatch spacing, and laser power are used. Only values of layer thickness vary, from 50 micrometers to 20 micrometers. (mod. Chen et al. 2018, p. 952)

As it can be observed from Figure 16, only values of layer thickness are varying. Largest value of surface roughness 12.3 µm occurs when value of *VED* of 46 J/mm^3 (layer thickness of 50 µm) is used, because the melt pool is not large enough and the unmolten powder remain on the track. In addition, the melt pool spatters the unmolten powder. The surface roughness values decrease till 3.5 µm when *VED* has value of 114 J/mm^3. On the contrary, values of surface roughness decrease when the values of layer thickness decrease. When the thinnest layer thickness, 20 µm, is used the value of surface roughness is the smallest, 3.50 µm. This is because the melt pool is now large enough to reach the previously molten layer so there is no unmolten powder remaining on the scan track and the melt pool does not spatter it.

6.2 Changes in microstructure

Changes in density can be measured for example by porosity rate. According to Amlou et al. (2017, p. 537), porosity rate is "considered as the percentage of void spaces in a material over the total volume". The microstructure changes are dependent on the quality and size of the melt pool. Moussaoui et al. (2018, p.185) found that *VED* values effect on the porosity rate of Inconel 718 fabricated by L-PBF. The results can be seen in Figure 17.

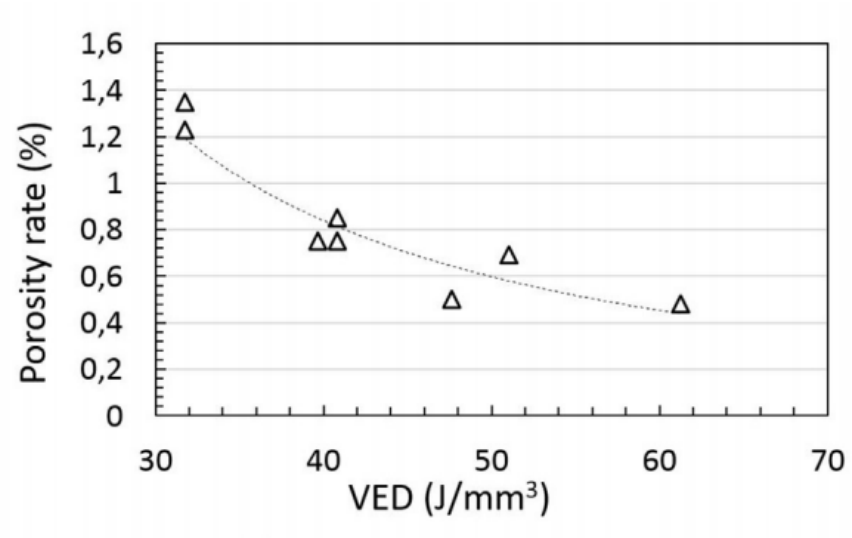

Figure 17. Porosity of Inconel 718 fabricated by L-PBF as function of *VED* (Moussaoui et al. 2018, p.185).

As it can be seen in Figure 17, porosity rate increases as function of *VED*. porosity rate decreases from 1.2 % to 0.5 % while *VED* values increase from 30 J/mm^3 to 50 J/mm^3. Because if *VED* value is too small, the porosity rate is high as the melt pool is not large enough (see Figure 8d). When *VED* values are increased, the melt pool is larger and is in better contact with previously molten layer (see Figure 8a). The formation of pores is illustrated in Figure 11. The correlation between porosity rate and *VED* can be noticed, because the more energy is brought to Inconel 718 the better the material melts. When the material is molten enough, voids and defects are less likely to occur. In addition, Feng et al. (2018, p. 482) found that voids can be formed in the overlapping areas of the melt pools, but often this kind of voids are smaller than voids formed by a low *VED*. (Gu & Jia 2013a, p. 716; Gu & Jia 2013b, p. 163; Moussaoui et al. 2018, p.185.)

6.3 Changes in mechanical properties

Mechanical properties are limited into tensile properties in this thesis due to time limitation. Feng et al. (2019 pp. 482–488) noticed that linear energy density (relation between laser power and scanning speed) has an impact on tensile properties of Inconel 718 manufactured by L-PBF. Based on the results of Feng et al. (2019, p.485) ultimate tensile strength is represented as function of linear energy density in Figure 18.

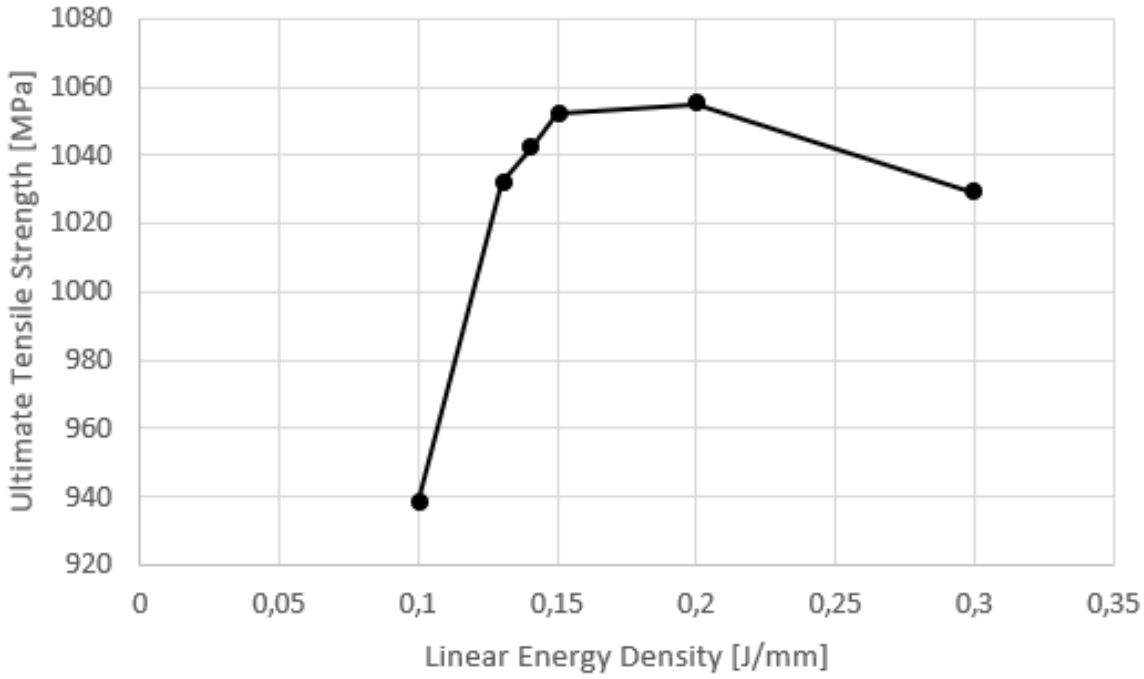

Figure 18. Ultimate tensile strength as a function of linear density when Inconel 718 is manufactured by L-PBF (mod. Feng et al. 2018, p.485*).*

As Figure 18 shows, maximum value of tensile strength occurs when linear energy density is 0.2 J/mm. When values of linear energy density of 0.1-0.2 J/mm are used, tensile strength values increase, because the more energy is brought to melting of Inconel 718. This leads to the better melting of the material and the better values of tensile strength too. Because when there is lack of melting in the material, pore formation is strong, and it starts to have effect on mechanical properties, such as decrease in ultimate tensile strength. (Chen et al. 2017, p. 104). When maximum value of tensile strength is reached with linear energy density value of 0.2 J/mm, tensile strength value is decreasing as linear energy density increases. Therefore, after the peak value of 0.2 J/mm, the material melts too much and harmful phenomena as vaporization of the material starts to occur. (Feng et al. 2018, p.485.) This phenomenon is illustrated in Figure 13.

7 DISCUSSION AND CONCLUSIONS

It is estimated that L-PBF process has over 110 parameters which affect this process. Therefore, parameters of L-PBF can be categorized in various ways. Aim of this thesis is to introduce main input process parameters and their effects on the quality of Inconel 718 manufactured by L-PBF.

This thesis introduces two different divisions of categorizing the parameters of L-PBF. Laser beam and material interaction model (see Figure 6) defines categorization of parameters based on their location in laser beam and material interaction. (Piili 2019; Piili 2012, p. 114.) The Ishikawa diagram (see Figure 8) divides the parameters into groups and subgroups by the type of parameter and their effect-cause relation. Usually, there are 4-6 groups which defines the type of a parameter and their effect-cause relation. Ishikawa diagram does not take into account effect of parameters in relation to desired property, such as final quality of workpiece. (Carty et al. 2018, p. 29.)

Volumetric energy density (*VED*) is selected as main parameter to be considered in this thesis as it combines most relevant input parameters, such as laser power, scanning speed, hatch spacing and layer thickness. *VED* is also widely used in literature. (Bertoli et al. 2017 p. 331; Gong et al. 2013, p. 474; Emmelmann et al. 2016, p. 372; Gu 2015, p. 60; Guo et al. 2018, p. 483.) Equation for calculating *VED* is introduced in Equation 1. Figure 20 represents the overview of the harmful defects in the different laser beam and material interaction zones.

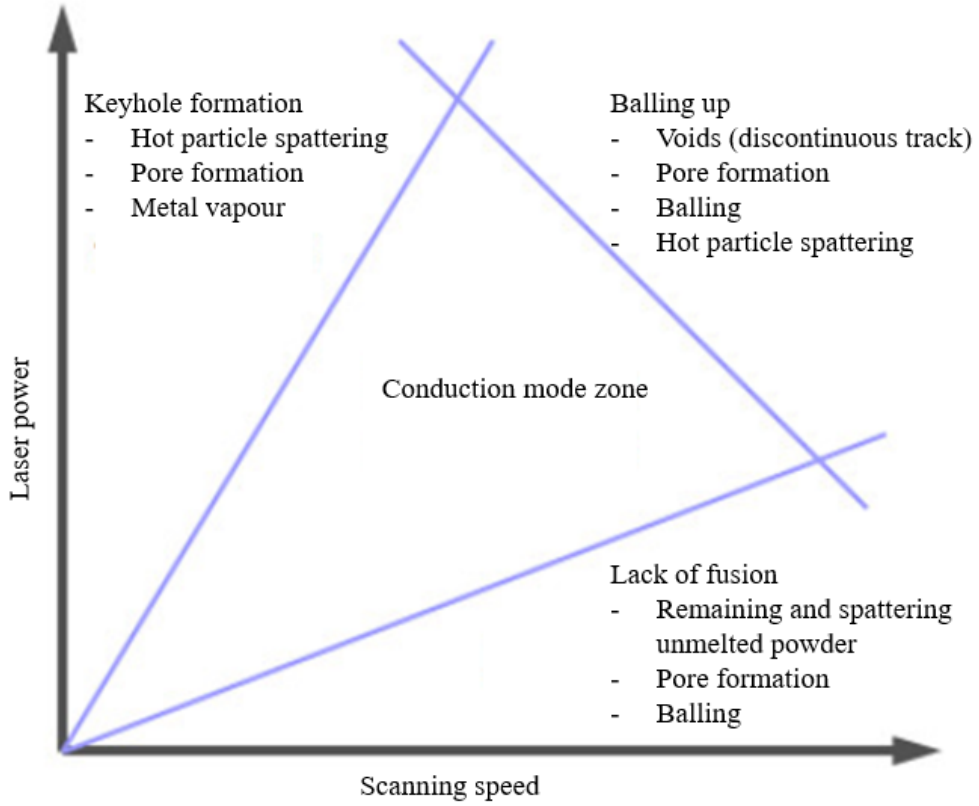

Figure 20. Overview of the harmful defects in the different laser beam and material interaction zones (mod. Saunders 2017).

Main input parameters when Inconel 718 is manufactured by L-PBF have direct effect on characteristics of melt pool. If melt pool loses its stability and starts to roil and spattering, different kind of defects start to occur, such as balling and porosity formation. (Qi et al. 2017, p. 258)

Optimum values of *VED* need to be defined when manufacturing Inconel 718 by L-PBF. Too low values of *VED* cause lack of fusion (see Figure 11d) (Saunders 2017). As it can be observed from Figure 20, when the laser beam and material interaction zone is lack of fusion, keyhole formation or balling up, harmful defects occur. Interaction zone is lack of fusion, when used value of scanning speed is too large and laser power is small. The laser beam travels too fast on the powder bed and unmolten powder remain on the track leading to weak tensile strength, high surface roughness and poor density of a part (Chen et al. 2017, p. 104). Balling up occurs, when used scanning speed and laser power is too high i.e. large value of *VED* leading to unstable melt pool (see Figure 14) and resulting voids on the scan track.

Values of tensile strength decreases more when the interaction zone is lack of fusion or balling than keyhole mode. Also, the molten tracks are in the balling up zone discontinuous which worsen the tensile properties. Keyhole phenomena (see Figure 13) is the result of too large value of laser power and too slow scanning speed. (Saunders 2017.) Keyhole phenomena, such as lack of fusion and balling, are also harmful by having a tendency of porosity forming on previously molten, and solidified, layers (Qi et al. 2017, p. 258; Saunders 2017). The porosity itself reduces the desirable characteristics of Inconel 718 manufactured by L-PBF (Gu & Jia 2013a, p. 716; Gu & Jia 2013b, p. 163; Moussaoui et al. 2018, p.185).

The number of found scientific articles and studies relating the topic of this thesis is small (see Figure 3). Because of this, it is obvious that this issue needs further studies, such as clarification and more detailed preliminary studies of effect of process parameters to quality of Inconel 718 manufactured by L-PBF.

Based on literature survey carried out for this thesis, it is concluded that values of *VED* as only observing parameter might not be most suitable parameter to describe effect of main process parameters to quality of an end-product when Inconel 718 is manufactured by L-PBF. This is because it is difficult to compare *VED* values found from different studies without knowing how value of *VED* is calculated, *VED* is useful parameter if its calculation is known. Namely, many research studies found from literature do not define which parameters are used for calculation of *VED*.

It was concluded in this thesis that as *VED* can be calculated many ways, it might be quite problematic for comparisons, if it is not known exactly how *VED* is defined. It was also concluded in this study that as *VED* is experimental value, it can be easily used for preliminary studies, but for further studies all parameters need to be taken into account.

8 SUMMARY

Aim of this thesis is to find the effect of the most common input parameters on the properties of Inconel 718 manufactured by L-PBF, based on literature survey.

This study was carried out in co-operation with company Etteplan and research group of Laser Material Processing of LUT University as a part of Metal 3D Innovations (Me3DI) project funded by European Regional Development Fund. Aim of Metal 3D Innovations-project (Me3DI) is to form industrial knowhow cluster of metallic 3D printing to South Karelia. This cluster will enhance utilization of additive manufacturing (3D printing) of metallic materials. This project is funded by European Regional Development Fund. Project started in 1.9.2018 and ends in 31.12.2020. Research group of Laser Materials Processing and research group of Steel Structures of LUT University and industrial companies are participating into this project.

Based on literature findings, it was decided in this thesis to focus on the volumetric energy density, *VED*, which combines in calculation scanning speed, laser power, hatch spacing and layer thickness. These four parameters are most common process parameters based on literature.

Effect of the main input parameters and *VED* on Inconel 718 manufactured by L-PBF was studied by exploiting a laser beam and material interaction division. The division has four interaction zones: conduction mode zone, lack of fusion, keyhole formation and balling up. It was noticed that when using a large values of scanning speed and laser power the laser beam and material interaction mode is balling up. In balling up, the formed track is discontinuous due to unstable melt pool causing poor tensile properties and high surface roughness and porosity rate. Large value of *VED* (with high laser power and low scanning speed) causes porosity formation into previous molten layers and hot metal particle spattering. This laser beam and material interaction mode is keyhole effect mode. Lack of fusion interaction mode occurs when low *VED* values are used. In this mode, the molten layers do not form a bond between each other because the melt pool is too tiny. Also, because all the powder does not melt, some unmolten powder remains on between the layers. Because

of those defects, lack of fusion results a significant drop in tensile properties and high porosity rate and surface roughness. When the input parameters are controlled well, and no harmful phenomena occur, is the zone called conduction mode zone.

9 FURTHER STUDIES

When conducting this thesis, it was noticed that calculation of *VED* and parameters used for this calculation needs to be defined well. Many articles based on literature survey do not define these values, and it is causing problems when conclusions need to be carried out. Suggestions for further studies are:

- Preliminary, fundamental studies of effect of process parameters on quality of Inconel 718. These studies should introduce thoroughly all parameters used for calculation of *VED*.
- Determining the parameter interface for different laser beam and material interaction zones.
- Creating a new energy density model or improving the old one to the form which allows better comparing the values between different studies.

LIST OF REFERENCES

Amlou, O., Koutiri, I., Pessard, E., Peyre & P., Terris, T. 2017. Influence of SLM process parameters on the surface finish, porosity rate and fatigue behavior of as-built Inconel 625 parts. In: Journal of Materials Processing Tech C, Volume 255. Pp. 536–546.

Arrazola, P.J., Garay, A., Germain, G., Giraud, E., Iturbe, A., Hormaetxe, E. & Ostolaza, K. 2016. Mechanical characterization and modelling of Inconel 718 material behavior for machining process assessment. In: Materials Science & Engineering A, Volume 682. Pp. 441–453.

Alfieri, V., Argenio, P., Caiazzo, F. & Corrado, C. 2017. Laser powder-bed fusion of Inconel 718 to manufacture turbine blades. In: The International Journal of Advanced Manufacturing Technology, Volume 93, Pp. 4023–4031.

Arroyave, R., Elwany, A., Franco, B., Karaman, I., Mahmoudi, M. & Tapia, G. 2018. On the printability and transformation behavior of nickel-titanium shape memory alloys fabricated using laser powder-bed fusion additive manufacturing. In: Journal of Manufacturing Processes, Volume 35. Pp. 672–680.

Ashral, M., Gibson, I. & Rashed, M. 2018. CHALLENGES AND PROSPECTS OF 3D PRINTING IN STRUCTURAL ENGINEERING. In: 13th International Conference on Steel, Space and Composite Structures.

Atwood, A., Bodey, A., Lee, P., Leung, C., Jones, J., Marussi, T., Towrie, M., Val Garcia, J. & Withers, P. 2018. Laser-matter interactions in additive manufacturing of stainless steel SS316L and 13-93 bioactive glass revealed by in situ X-ray imaging. In: Additive Manufacturing, Volume 24. Pp. 647–657.

Austbø, H., Hansen, V., Lysne, V. H., Sjolyst-Kverneland, A. & Tucho, W. M. 2018. Investigation of effects of process parameters on microstructure and hardness of SLM manufactured SS316L. In: Journal of Alloys and Compounds 740. Pp 910-925.

Bertoli, U. S., Delplanque, J. P. R., Matthews, M. J., Schoenung, J. M., & Wolfer, A. J. (2017). On the limitations of volumetric energy density as a design parameter for selective laser melting. In: Materials & Design 113. Pp. 331-340.

Borisov, E., Masaylo, D., Orlov, A., Polozov, I., Popovich, A. & Sufiiarov, V. 2016. The effect of layer thickness at selective laser melting. In: Procedia Engineering, Volume 174. Pp. 126–134.

Carty, C., Martinez, D., Mirnajafi, A. & Stewart, R. 2018. Application of quality by design for 3D printed bone prostheses and scaffolds. In: PloS one, Volume 13.

Chua, C., Dong, Z., Liu, Z., Loh, L., Sing, S., Yap, C. & Sing, S. 2015. Review of selective laser melting: Materials and applications. In: Applied physics reviews 4, Volume 2.

Cong, W., Kim, H., Liu, Z., Wang, X., Zhang, H. & Zhou, Y. 2018. Investigations of Energy Density Effects on Forming Accuracy and Mechanical Properties of Inconel 718 Fabricated by LENS Process. In: Procedia Manufacturing, Volume 26. Pp. 731–739.

Chen H., Dai, D., Gu, D., Shi, Q., Xia, M. & Yu, G. 2017. Porosity evolution and its thermodynamic mechanism of randomly packed powder-bed during selective laser melting of Inconel 718 alloy. In: International Journal of Machine Tools and Manufacture. Volume 116. Pp. 96–106.

Chen, Z., Luu, D. N., Nai, S. M. L., Nguyen, Q. B., Wei, J. & Zhu, Z. (2018). The role of powder layer thickness on the quality of SLM printed parts. Archives of Civil and Mechanical Engineering, 18(3), 948-955.

DebRoy, T. & Mukherjee, T. 2018. Mitigation of lack of fusion defects in powder bed fusion additive manufacturing. In: Journal of Manufacturing Processes 36. Pp. 442–449.

Donmez, A., Lane, B., Lopez, F., Mekhontsev, S. & Vlasea, M. L. 2015. Development of powder bed fusion additive manufacturing test bed for enhanced real-time process control. In: Proceedings of the International Solid Freeform Fabrication Symposium. Pp. 527–539.

Gibson, I., Rosen, D. & Stucker, B. 2015. Additive Manufacturing Technologies: 3D Printing, Rapid Prototyping, and Direct Digital Manufacturing. Second edition. New York: Springer. 498 p.

Gu, H., Gong, H., Pal, D., Rafi, K., Starr, T., & Stucker, B. (2013, August). Influences of energy density on porosity and microstructure of selective laser melted 17-4PH stainless steel. In: Solid Freeform Fabrication Symposium. Pp. 474–489

Gu, D. 2015. Laser additive manufacturing of high-performance materials. Berlin: Springer. 311 p.

Gu, D. & Jia, Q. 2013a. Selective laser melting additive manufacturing of Inconel 718 superalloy parts: Densification, microstructure and properties. In: Journal of Alloys and Compounds, Volume 585. Pp. 713–721.

Gu, D. & Jia, Q. 2013b. Selective laser melting additive manufactured Inconel 718 superalloy parts: High-temperature oxidation property and its mechanisms. In: Optics & Laser Technology, Volume 62. Pp. 161–171.

Gu. D & Shen. Y. 2009. Effects of processing parameters on consolidation and microstructure of W–Cu components by DMLS. In: Journal of Alloys and Compounds 1-2, Volume 473. Pp. 107-115.

Guo, Y. L., Jia, L. N., Kong, B., Huang, Y. L., & Zhang, H. 2018. Energy Density Dependence of Bonding Characteristics of Selective Laser-Melted Nb–Si-Based Alloy on Titanium Substrate. In: Acta Metallurgica Sinica. Pp. 477–486.

Emmelmann, C., Herzog, D., Seyda, V.& Wycisk, E. 2016. Additive manufacturing of metals. Acta Materialia 117. Pp. 371-392.

Feng, T., Feng, Y., Hu, Y., Kang, J., Wang, X., Wu, P. & Yi, J. 2019. Effect of laser energy density on the microstructure, mechanical properties, and deformation of Inconel 718

samples fabricated by selective laser melting. In: Journal of Alloys and Compounds, Volume 786. Pp. 481–488.

Korpela, M. 2019. Material needs of Finnish metal and mechanical engineering industry from the perspective of additive manufacturing. 102 p.

Li, R., Liu, J., Shi, Y., Wang, L., & Jiang, W. 2012. Balling behavior of stainless steel and nickel powder during selective laser melting process. In: The International Journal of Advanced Manufacturing Technology 9-12, Volume 59. Pp. 1025–1035.

Liliana, L. 2016. A new model of Ishikawa diagram for quality assessment. In: IOP Conference Series: Materials Science and Engineering 1, Volume 161. Pp. 1–6.

Milewski, J. 2017. Additive Manufacturing of Metals. Santa Fe: Springer. 258 p.

Moussaoui, K., Mousseigne, M., Rezai, F. & Sultan, T. 2018. Effects of Selective Laser Melting additive manufacturing parameters of Inconel 718 on porosity, microstructure and mechanical properties. In: Materials Science and Engineering A. Volume 735. Pp. 182–190.

Nai, M., Nguyen, Q., Sun, C., Wei, J., Zhou, W. & Zhu, Z. 2017. Characteristics of Inconel Powders for Powder-Bed Additive Manufacturing. In: Engineering 5. Volume 3. Pp. 695–700.

Piili, H. Docent. LUT-University. Lappeenranta. Skype interview 15.2.2019. Interviewer Kalle Kohtanen.

Piili, H. 2012. Characterisation of Laser Beam and Paper Material Interaction. 265 p.

Qi, T., Zhu, H., Zhang, H., Yin, J., Ke, L., & Zeng, X. 2017. Selective laser melting of Al7050 powder: Melting mode transition and comparison of the characteristics between the keyhole and conduction mode. In: Materials & Design 135. Pp. 257–266.

Saunders, M. 2018. Spatter matters! [Referred 11.6.2019]. Available: https://www.linkedin.com/pulse/spatter-matters-marc-saunders

Saunders, M. 2017. X marks the spot - find ideal process parameters for your metal AM parts. [Referred 11.6.2019]. Available: https://www.linkedin.com/pulse/x-marks-spot-find-ideal-process-parameters-your-metal-marc-saunders

Special Metals. Inconel alloy 718 [web document]. Available: http://www.specialmetals.com/assets/smc/documents/inconel_alloy_718.pdf

Wang, D., Wu, S., Fu, F., Mai, S., Yang, Y., Liu, Y., & Song, C. 2017. Mechanisms and characteristics of spatter generation in SLM processing and its effect on the properties. In: Materials & Design 117. Pp. 121−130

Wohlers, T., Campbell, I., Diegel, O., Kowen, J. 2018. Wohlers Report 2018: 3D Printing and Additive Manufacturing State of the Industry Annual Worldwide Progress Report. Colorado, USA: Wohlers Associates. 343 p.

Wohlers, T., Campbell, I., Diegel, O., Kowen, J. 2019. Wohlers Report 2019: 3D Printing and Additive Manufacturing State of the Industry Annual Worldwide Progress Report. Colorado, USA: Wohlers Associates. 369 p.